Since in fact λ_D is very small, the left-hand side of Eq. (11) is negligible in the absence of thermal gradients. We then see that a potential gradient, and hence a resistance, is possible in a superconductor, but only in association with a time dependence of Ψ. Such a time dependence can occur by acceleration of a current, but seldom will; quite commonly, however, it is effected by the flow of magnetic vortex lines through a sample, since the passage of one vortex between two points requires a change of 2π in the relative phase of Ψ at those points.

Finally, we note that our basic equations are (4) and (9) and that the GL charge equation (11) follows from them. Furthermore, the derivation of (9) must be regarded as phenomenological because of the focus of attention on a "small" bit of superconductor in equilibrium. The present arguments do not include a specification of a minimum size for such a bit, and hence do not give a scale of lengths over which Eqs. (9) and (11) can be expected to hold. In fact, the more fundamental Green's function derivation of Eqs. (11) and (12) contains the requirement that disturbances be slowly varying in both space and time.

It is also worth noting that the GL equation (12) together with Eq. (4) may be used for a very compact derivation of a previously known result concerning the thermopower of a superconductor.[7] If the phase of the order parameter is $-2\mu t$, then the time derivative of the supercurrent is

$$\partial j/\partial t=(\rho_s e/m)(-\nabla\mu+eE). \tag{13}$$

Equation (13) shows that the emf in a closed circuit must be zero under conditions of zero current, and hence proves that a superconductor has zero thermopower.

We wish to thank Professor Stephen and Professor Suhl for informative conversations, and for supplying us with a copy of their manuscript prior to publication.

[7] J. M. Luttinger, Phys. Rev. **136**, A1481 (1964).

PHYSICAL REVIEW VOLUME 138, NUMBER 4A 17 MAY 1865

Low-Field de Haas–van Alphen Effect in Ag

A. S. Joseph and A. C. Thorsen
North American Aviation Science Center, Thousand Oaks, California
(Received 21 December 1964)

Detailed studies of the de Haas–van Alphen (dHvA) effect in Ag single crystals have been carried out with a high-sensitivity torque magnetometer in steady fields up to 40 kG. The angular variations of all of the pertinent dHvA frequencies were determined to better than 0.1%. We were able to achieve this precision by observing oscillations in the torque as the magnetic field was rotated with respect to the samples at a fixed magnetic field. More data have been obtained on the new low-frequency oscillations which we recently reported, and evidence is presented which suggests that these oscillations may be associated with a difference frequency between two extremal belly orbits.

INTRODUCTION

THE detailed study of the de Haas–van Alphen (dHvA) effect in Ag by Schoenberg[1] showed that the Fermi surface (FS), like that in Cu, could be represented by a single sheet which is multiply connected along the ⟨111⟩ directions. These measurements provided sufficient information about the FS to allow a mathematical description[2] of the shape of the surface, although several features of the surface could not be investigated in detail by pulsed-magnetic-field techniques. In an attempt to complete the experimental picture we have undertaken a systematic study of the dHvA effect in Ag by means of the steady-field torsion-balance method. In the initial phase of this study a new low-frequency oscillation F_c was observed[3] which appeared to be inexplicable in terms of the above model of the FS, and was therefore tentatively attributed to a small pocket of electrons in the second Brillouin zone, centered at the symmetry point L. Further studies of these oscillations have cast some doubt on this interpretation and have led to an alternative explanation based on a nonlinear oscillatory effect of the type first considered by Shoenberg.[1,4] In effect, electrons in the metal experience a field $B=H_0+4\pi M$ rather than the applied field H_0. When M, and hence B, is oscillatory, Shoenberg has shown that the dHvA oscillations have an unusually large harmonic content. He also pointed out that if more than one dHvA frequency is present, sum and difference frequencies may be generated. Accordingly, the low frequency F_c may arise as a difference frequency between two dHvA oscillations rather than from a new segment of the FS. The origin of F_c can thus be traced to the existence of *two* extremal belly orbits, whose

[1] D. Shoenberg, Phil. Trans. Roy. Soc. (London) **A255**, 85 (1962).
[2] D. J. Roaf, Phil. Trans. Roy. Soc. (London) **A255**, 135 (1962).
[3] A. S. Joseph and A. C. Thorsen, Phys. Rev. Letters **13**, 9 (1964).
[4] A. B. Pippard, Proc. Roy. Soc. (London) **A272**, 192 (1963).

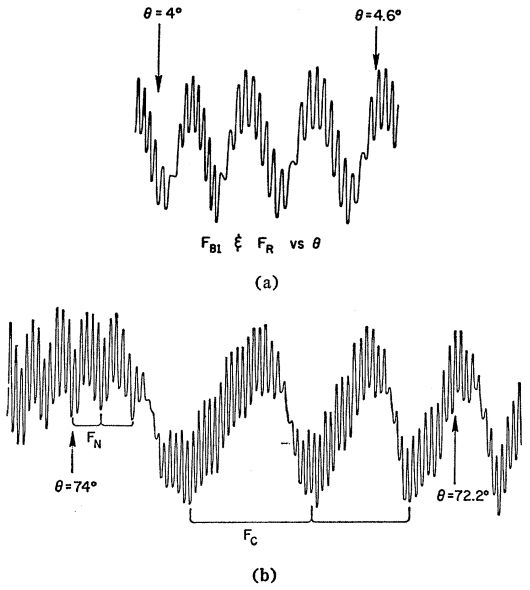

FIG. 1. (a) Typical examples of torque versus orientation at constant magnetic field showing the change in phase of the rosette and belly in the angular range $4.0°<\theta<4.6°$. Here the phase of the rosette is varying more rapidly than the phase of the belly. Note that there is a beat in the faster oscillations which remains in phase with the slower oscillations. (b) Variation in the phases of the belly, neck, and F_c in the angular range $72°<\theta<74°$. The fast oscillations are associated with the phase of the belly and are beating with the same periodicity as the low-frequency F_c. The oscillations associated with the neck are weak in this region owing to the vanishing of the spin-splitting factor, but become very large on either side of this region.

areas differ by an amount proportional to F_c. In order to find further evidence bearing on this possibility we have re-examined the belly oscillations by observing the torque as a function of field orientation in constant magnetic fields. Angular variations of the belly frequencies were determined to about one part in 10^4 and their angular ranges were measured to within 0.2°. For the sake of completeness this technique was also used to determine with comparable accuracy the angular variations of the other pertinent frequencies in Ag.

TABLE I. F_{B1}, F_{B2}, F_C, F_R, and F_D (in units of 10^8 G) in the (100) plane. The angle φ is measured from [001] axis.

φ	F_{B1}	F_R	φ	F_{B1}	F_C	F_{B2}	φ	F_D
0	4.7708	1.9661	18.1	4.7592			37.1	2.1396
1.1	4.7707	1.9678	19.1	4.7627			38	2.1063
2.1	4.7699	1.9724	20.1	4.7671			39	2.0800
3.1	4.7687	1.9802	21.1	4.7725			40	2.0590
4.1	4.7672	1.9908	22.1	4.7790			41	2.0430
5.1	4.7655	2.0051	23.1	4.7859			42	2.0306
6.1	4.7636	2.0236	24.1	4.7938			43	2.0230
7.1	4.7616	2.0465	25.1	4.8030			44	2.0180
8.1	4.7595	2.0739	26.1	4.8130			45	2.0163
9.1	4.7574		27.1	4.8242				
10.1	4.7556		28.1	4.8364	0.0573	4.7791		
11.1	4.7542		29.1	4.8494	0.0435	4.8059		
12.1	4.7531		30.1	4.8638	0.0303	4.8335		
13.1	4.7524		31.1	4.8787	0.0194	4.8593		
13.4	4.7523		32.1	4.8949	0.0108	4.8841		
14.1	4.7527		33.1	4.9136	0.0045	4.9091		
15.1	4.7533		34.1	4.9332	0.0005	4.9324		
16.1	4.7545		35.1	4.9553				
17.1	4.7565		36.1	4.9881				

TABLE II. F_{B1}, F_{B2}, F_C, and F_R (in units of 10^8 G) in the $(1\bar{1}0)$ plane. The angle θ is measured from the [001] axis.

θ	F_{B1}	F_R	θ	F_{B1}	θ	F_{B1}	F_{B2}	F_C
0	4.7708	1.9661	10	4.7518	20	4.7376	4.6669	0.0707
1	4.7706	1.9680	11	4.7490	21	4.7391	4.6851	0.0540
2	4.7699	1.9719	12	4.7462	22	4.7413	4.7051	0.0362
3	4.7688	1.9796	13	4.7437	23	4.7443	4.7224	0.0219
4	4.7671	1.9922	14	4.7415	24	4.7481	4.7367	0.0114
5	4.7650	2.0076	15	4.7397	25	4.7531	4.7484	0.0047
6	4.7628	2.0294	16	4.7381	26	4.7590	4.7582	0.0008
6.6		2.0524	17	4.7373	27	4.7672		
7	4.7601		18.1	4.7367	28.1	4.7807		
8	4.7576		19	4.7368				
9	4.7546							

EXPERIMENTAL

The details of the null-deflection torsion balance and auxilliary apparatus have been discussed elsewhere.[5] An added modification included the installation of a motor drive on the 22-in. Varian magnet so that it could be rotated at angular velocities up to 5° per minute. The changes in dHvA frequencies with angle were determined by observation of the variation in phase (defined as the ratio F/H_0, where F is the dHvA frequency and H_0 is the magnetic field) as the magnet was rotated at some constant field. A typical recording of a rotation diagram is presented in Fig. 1 (a) showing the change in phase of the belly and rosette in the $(1\bar{1}0)$ plane. The various oscillating terms in Ag were followed in this fashion in both the $(1\bar{1}0)$ and (100) planes.

The silver samples, grown by W. Allred of the Bell and Howell Research Center, had residual resistivities

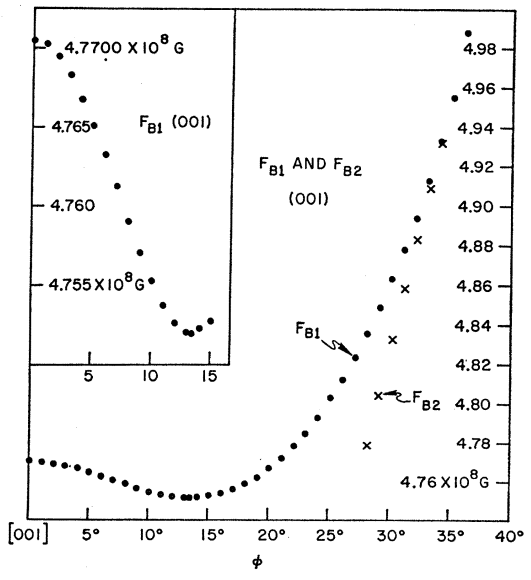

FIG. 2. Plots of the dHvA frequencies of the belly oscillations F_{B1} and F_{B2} in the (100) plane as functions of the angle φ between the field and the [001] axis. In the inset F_{B1} is plotted for $0<\varphi<15°$ on an expanded scale to illustrate the high accuracy in the relative variation in F_{B1}.

[5] A. S. Joseph and A. C. Thorsen, Phys. Rev. 133, A1546 (1964), and references therein.

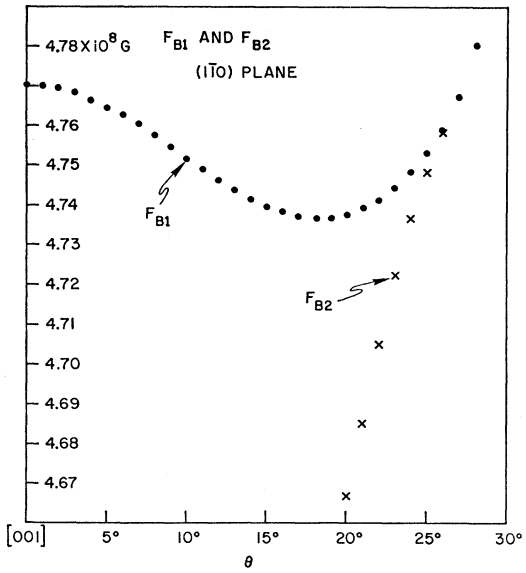

FIG. 3. Plots of the dHvA frequencies of the belly oscillations F_{B1} and F_{B2} near the [001] axis in the (1$\bar{1}$0) plane as functions of θ.

of about 800. They were carefully spark-cut and oriented within 0.5° in the (1$\bar{1}$0) and (100) planes.

RESULTS AND DISCUSSION

The angular variations of the belly (F_{B1}), dog's bone (F_D), four-cornered rosette (F_R), and neck (F_N) frequencies are shown in Figs. 2–7 and are tabulated in Tables I–V. In all cases the angle θ is measured from the [001] axis in the (1$\bar{1}$0) plane and φ is measured from the [001] axis in the (100) plane. The absolute values of the frequencies F_{B1}, F_D, and F_R were determined by counting approximately 2100, 600, and 1200 oscillations, respectively, yielding an accuracy which we estimate to be better than 1.5%. The relative accuracy is determined primarily by the phase of the particular set of oscillations, those oscillations with the highest phase having the highest accuracy. This leads to a relative accuracy of $\approx$0.01% for F_{B1} and $\approx$0.1% for F_N. In regions where comparison is possible, the frequency values are generally found to be within the limits of error of those determined previously.[1]

TABLE III. F_{B1}, F_{B2}, and F_C (in units of 10^8 G) in the (1$\bar{1}$0) plane. The angle θ is measured from the [001] axis. The angle $\theta=54.75$ corresponds to H along the [111] axis.

θ	F_{B1}	F_C	F_{B2}	θ	F_{B1}	F_C	F_{B2}
42.2	4.7144			60	4.6284	0.0329	4.5955
43.0	4.7014		4.7014	61	4.6354	0.0290	4.6064
44	4.6858	0.0001	4.6857	62	4.6429	0.0253	4.6176
45	4.6722	0.0008	4.6714	63	4.6516	0.0224	4.6292
46	4.6589	0.0029	4.6560	64	4.6616	0.0194	4.6422
47	4.6489	0.0063	4.6426	65	4.6722	0.0164	4.6558
48	4.6391	0.0100	4.6291	66	4.6844	0.0138	4.6706
49	4.6320	0.0156	4.6164	67	4.6977	0.0111	4.6866
50	4.6259	0.0214	4.6045	68	4.7115	0.0089	4.7026
51	4.6211	0.0271	4.5940	69	4.7269	0.0064	4.7205
52	4.6173	0.0343	4.5830	70	4.7431	0.0042	4.7389
53	4.6146	0.0431	4.5715	71	4.7606	0.0025	4.7581
54	4.6129	0.0522	4.5607	72	4.7793	0.0017	4.7776
54.75	4.6126	0.0552	4.5572	73	4.7987		
56.0	4.6135	0.0500	4.5635	74	4.8202		
57	4.6156	0.0455	4.5701	75	4.8421		
58	4.6185	0.0412	4.5773	76.3	4.8733		
59	4.6230	0.0374	4.5856				

TABLE IV. F_N (in units of 10^8 G) in the (1$\bar{1}$0) plane. The angle θ is measured from the [001] axis.

θ	F_N	θ	F_N	θ	F_N
28.6	0.21614	46	0.09272	65	0.09474
29.3	0.19244	47	0.09168	66	0.09622
30	0.17243	48	0.09077	67	0.09793
31	0.15620	49	0.09000	68	0.09985
32	0.14405	50	0.08937	69	0.10204
33	0.13458	51	0.08886	70	0.10456
34	0.12779	52	0.08850	71	0.10746
35	0.12186	53	0.08825	72	0.11077
36	0.11696	54.75	0.08811	73	0.11457
37	0.11281	56.5	0.08839	74	0.11907
38	0.10922	58	0.08887	75	0.12432
39	0.10610	59	0.08930	76	0.13062
40	0.10333	60	0.08984	77	0.13832
41	0.10090	61	0.09051	78	0.14800
42	0.09879	62	0.09133	79	0.16070
43	0.09693	63	0.09231	80	0.17770
44	0.09530	64	0.09344	81	0.20067
45	0.09392			81.7	0.22417

The absolute value of the neck frequency along the [111] axis, also determined to $\pm$0.5%, agrees with the value reported earlier.[3] The relative angular change in F_N fits the theoretical expression reported in Ref. 3 to within 1% for $m_t/m_l=3.24\pm0.02$. We have compared

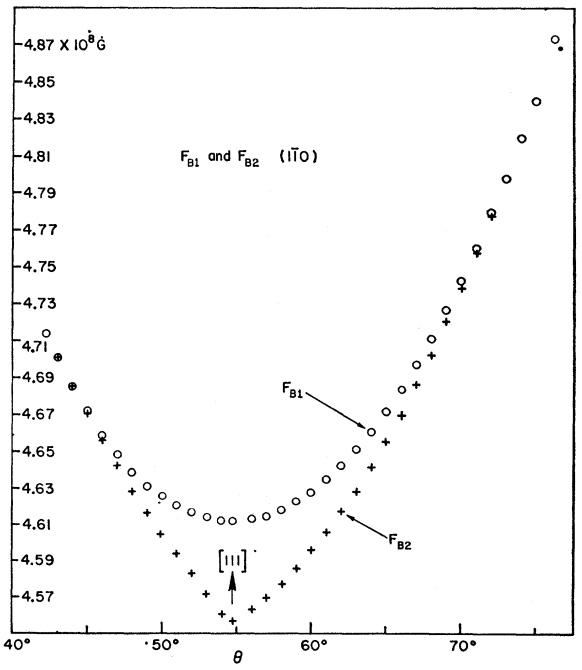

FIG. 4. Plots of the dHvA frequencies of the belly oscillations F_{B1} and F_{B2} near the [111] axis in the (1$\bar{1}$0) plane as functions of the angle θ, measured from the [001] axis.

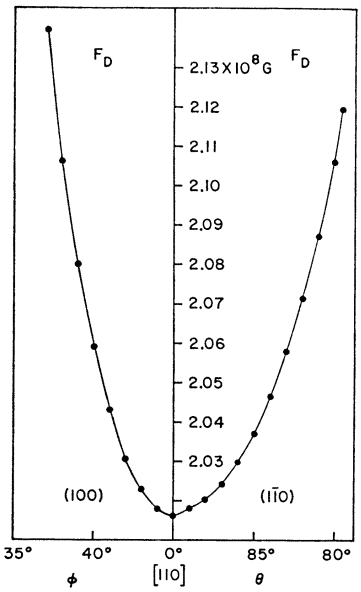

FIG. 5. Plots of the dHvA frequencies of the oscillations associated with the dog's bone in the (100) and (1$\bar{1}$0) planes as functions of φ and θ.

the ranges over which F_D and F_R are observable with the values calculated on the assumption that the necks are of circular cross section. For F_D the calculated ranges are 24° and 17° for the (1$\bar{1}$0) and (100) planes respectively, compared to the experimental values of 21.2° and 15.8°. The calculated maximum range for the rosette in the (100) plane is 16.5° compared to the experimental value of 16°.

The angular dependence and frequency values of the low-frequency oscillations F_c observed in Ag and reported in Ref. 3 have been verified in two separate crystals. An example of these low-frequency oscillations is shown in Fig. 8. In addition, other low-frequency oscillations (also designated as F_c) have been detected in another narrow region of the (1$\bar{1}$0) plane and over a range of 6° in the (100) plane. These results are listed in Tables I–III. The usual behavior of F_c, viz., the small ranges of observation, the rapid variation of frequency with angle, and the approach of the frequency to zero, strongly suggests that the oscillations are not associated with a closed segment of FS as previously suspected. The alternative explanation of these oscillations as a difference frequency arising from the interaction of two extremal belly orbits, was suggested independently by Gordon, Lomer, and Pippard.[6] The existence of two extremals in the belly should be manifested experimentally as beats in the belly oscillations. In most orientations where F_c was observed, plots of torque versus field showed no evidence of such beats even though several thousand oscillations could be counted. In contrast, the rotation diagrams did exhibit strong beats in the belly phase in some regions, as shown in Fig. 1 (b). These beat waists are indicative of another

[6] W. L. Gordon, W. M. Lomer, and A. B. Pippard (private communication).

TABLE V. F_D (in units of 10^8 G) in the (1$\bar{1}$0) plane. The angle θ is measured from the [001] axis.

θ	F_D
79.6	2.1194
80.0	2.1059
81.0	2.0872
82.0	2.0714
83.0	2.0580
84.0	2.0465
85.0	2.0371
86.0	2.0301
87.0	2.0241
88.0	2.0203
89.0	2.0178
90.0	2.0163

frequency term whose phase is changing at approximately the same rate with angle and may be associated with the other belly orbit F_{B2}. (Note that the distance between waists then corresponds to a change of one in the phase associated with F_c.) When the belly oscillations were observed as a function of field at an angle at which there occurred a beat waist in the phase, evidence of a long beat was discernible but consisted at most of the observation of a single beat waist. In Figs. 2–4 we show the values of F_{B2} as functions of θ and φ, calculated from the relation $F_{B2}=F_{B1}-F_c$. For $24°<\theta<26.5°$ and for $33°<\varphi<34°$ it was clear from the beat waists in the rotation diagrams that F_{B2} is less than F_{B1}. However for $42°<\theta<74°$ we could not definitely determine from a study of the beat waists if F_{B2} was larger or smaller than F_{B1}. In Fig. 3 we assume $F_{B1}>F_{B2}$. Such an assumption is consistent with the picture that F_{B1} is associated with a central orbit having a maximum area with respect to k_H (k_H is the

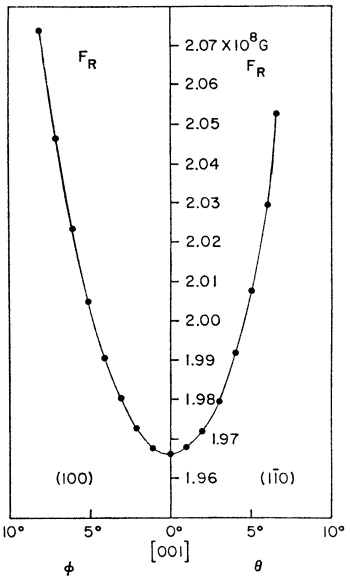

FIG. 6. Plots of the dHvA frequencies of the oscillations associated with the four-cornered rosette in the (100) and (1$\bar{1}$0) planes as functions of φ and θ.

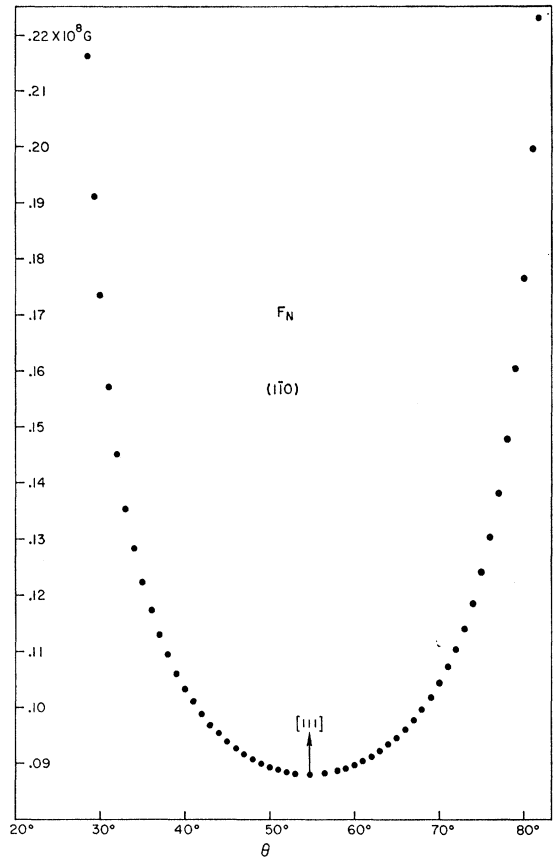

FIG. 7. Plot of dHvA frequencies of the oscillations associated with the neck in the (1$\bar{1}$0) plane as a function of θ.

wave vector in the direction of H) and F_{B2} is associated with a noncentral orbit of a slightly smaller area.[7]

Further evidence that F_c is due to nonlinear behavior in the magnetization was found in other unusual effects related to the amplitudes of the oscillations. Whenever two oscillatory terms occurred simultaneously, it was usually observed that the amplitude of one was modulated with the periodicity of the other. This modulation was evidence of a third oscillating term having a frequency equal to the difference between the two original terms. It is interesting to note that a difference frequency, once generated, can interact with another oscillating term to produce yet another frequency. An example of this was a modulation of the neck oscillations by F_c. These amplitude modulations occur in plots of torque versus angle [Fig. 1 (a)] as well as torque versus field.

A further consequence of nonlinear effects on the amplitude of the belly oscillations relates to the temperature dependence and was also observed in Be by Plummer *et al.*[8] For most orientations where effective mass measurements were made, a plot of $\ln(A/T)$ versus T (A = amplitude of the dHvA oscillations) was found to deviate from linearity, suggesting a saturation in the amplitude at low temperatures ($T \lesssim 1.6°\text{K}$). Since the effective mass is deduced from the slope of this line, mass values for the belly were obtained from the high-temperature region, $1.6°\text{K} < T < 2.17°\text{K}$, where the curve usually becomes linear. This effect probably accounts for the unusually low value of m^* found from the pulsed field measurements in Ag.[1] It is somewhat surprising that in the region $28° < \varphi < 26°$ where F_{B1}, F_{B2}, and F_c were observed, effective mass plots of the belly down to 1.12°K showed no evidence of saturation, whereas near the [111] and [001] axes, such plots showed no evidence of linearity even at higher temperatures. The effective-mass plots for the oscillations associated with other sections of the FS and also for the low-frequency oscillations showed little or no evidence for saturation at low temperatures. The effective-mass values derived from these measurements are given in Table VI.

The shape of the wave form of the belly oscillations was sometimes quite distorted and was indicative of rather high harmonic content. A sample recording of torque showing oscillations in the belly is shown in Fig. 9. The extreme distortion is probably similar to the sawtooth wave[8] observed in Be and was observed on occasion in both the (1$\bar{1}$0) and (100) planes. This distortion was not always reproducible.

A rather puzzling observation concerns the amplitude of F_c. These oscillations were quite strong and in general comparable to the neck and belly oscillations in amplitude. At low fields (in the vicinity of 20 kG) where the amplitude of F_{B1} vanished the low-frequency oscillations continued to exhibit appreciable amplitude and could be observed to much lower fields (typically $H \sim 18$ kG). This is unexpected in view of the interpretation that the low frequency is generated by two belly oscillations. Furthermore, it differs from the behavior of the difference frequency observed in Be.[8] A possible explanation may be that local field inhomogeneities (or field nonuniformity) in the sample could be large enough to dephase the contributions by different regions of the sample to the closely spaced (in field)

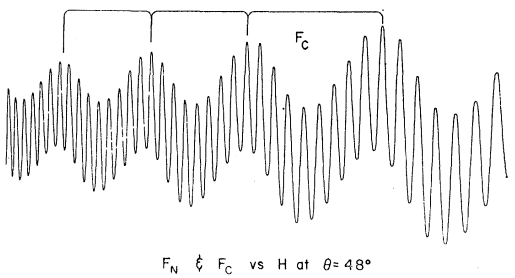

FIG. 8. Sample of the dHvA oscillations associated with F_c and F_N, recorded as functions of H, for $\theta = 48°$. The low-frequency oscillations correspond to F_c. Oscillations due to the belly are filtered out.

[7] D. Shoenberg has pointed out (private communication) that this assumption is consistent with Roaf's computations of Ag (Ref. 2).

[8] R. D. Plummer and W. L. Gordon, Phys. Rev. Letters **13**, 432 (1964).

TABLE VI. Effective-mass values for the belly, dog's bone, neck, and the low-frequency F_C. Unless otherwise noted, the accuracy of the belly and dog's-bone effective masses is ±3%, and the accuracy of the neck effective masses is ±6%. The plots for the belly effective mass taken at $\theta=50°$, 59°, and 64° exhibit strong saturation.

Belly (100)		Belly (1$\bar{1}$0)		Dog's Bone (100)		Neck (1$\bar{1}$0)		F_C (1$\bar{1}$0)	
φ	m^*/m_0	θ	m^*/m_0	φ	m^*/m_0	θ	m^*/m_0	θ	m^*/m_0
10.1	0.91	11	1.00	43.9	1.04	30.5	0.75	24	1.35±0.03
15.1	0.91	25	1.06	41.9	1.07	34.6	0.56	49	1.2 ±0.1
20.1	0.92	27.85	1.19	39.9	1.16	36.95	0.50	51	1.4 ±0.2
25.1	0.93	50	0.97±0.05			38.90	0.47	54	1.3 ±0.2
30.1	0.99	59	0.94±0.05			41.60	0.43		
33.1	1.07	64	0.97±0.05			45.60	0.41		
34.1	1.02	69	1.00			50.60	0.39		
		74	1.08			53.6	0.39		
						69.9	0.46		
						74.9	0.57		

belly oscillations. The contributions of each region of the sample to F_c, however, may well remain in phase due to the comparatively large spacing between these low-frequency oscillations.

CONCLUSIONS

We have presented in this paper the results of an accurate and detailed study of the dHvA effect in Ag. Tabulated values of the relative variations of belly frequencies, accurate to better than one part in 10^4, and variations in the neck, rosette, and dog's bone frequencies, accurate to better than one part in 10^3, should provide the basis for a more accurate analytical representation of the FS of Ag. Such a representation should shed interesting light on the plausibility of interpreting F_c as a difference frequency which is a consequence of the simultaneous existence of two extremal belly orbits. Evidence for such orbits has been presented above. Several other features of the data are as yet unexplained: (1) the nonreproducibility of the shape of the belly oscillations where large harmonic content is present; (2) the persistence of F_c at low fields where the belly oscillations have vanished; (3) the absence of saturation in the belly oscillations in the region of the (100) plane where F_c is observed.

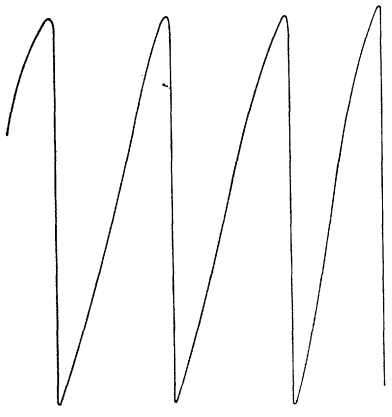

FIG. 9. Sample of the belly oscillations recorded as a function of H at $\varphi=33°$ where large harmonic content is evident.

Note added in proof. The frequencies F_{B1}, F_{B2}, F_R, and F_D listed in Tables I, II, III, and V have an absolute accuracy of 1.5%. A recheck of the magnetic field calibration has disclosed a shift of ≈250 G in the high-field region. This discrepancy results in an ≈1% shift in the above frequencies. For more accurate absolute values, the following frequencies should read:

$$F_{B1}=4.5665\times10^8 \text{ G} \quad \text{at} \quad \theta=54.75°,$$
$$F_{B1}=4.7231\times10^8 \text{ G} \quad \text{at} \quad \theta=0°, \quad \varphi=0°,$$
$$F_D=1.9961\times10^8 \text{ G} \quad \text{at} \quad \theta=90°, \quad \varphi=45°,$$
$$F_R=1.9464\times10^8 \text{ G} \quad \text{at} \quad \theta=0°, \quad \varphi=0°.$$

The frequencies at other angles can be calculated from the change in frequency with angle $(\Delta F/\Delta\theta, \Delta F/\Delta\varphi)$ which can be found from the tables, and which remains unchanged. These corrections lead to an absolute accuracy of ±0.5% for the above frequencies. The values of F_N and F_C given in Tables I–IV are correct as listed.

ACKNOWLEDGMENTS

The authors wish to thank W. M. Lomer, A. B. Pippard, W. L. Gordon, and D. Shoenberg for many helpful discussions and suggestions which led to the interpretation that F_c is a difference frequency between two belly orbits. We would also like to thank T. G. Berlincourt for many stimulating conversations and his continued interest in this work. We further acknowledge E. Gertner for his assistance in taking and plotting much of the data and P. C. Romo and D. G. Swarthout for orienting the samples.